Molecules and Cells

Hsa-miR-422a Originated from Short Interspersed Nuclear Element Increases *ARID5B* Expression by Collaborating with NF-E2

Woo Ryung Kim[1,2], Eun Gyung Park[1,2], Hee-Eun Lee[3], Sang-Je Park[3], Jae-Won Huh[3,4], Jeong Nam Kim[5], and Heui-Soo Kim[2,6,*]

[1]Department of Integrated Biological Science, Pusan National University, Busan 46241, Korea, [2]Institute of Systems Biology, Pusan National University, Busan 46241, Korea, [3]National Primate Research Center, Korea Research Institute of Bioscience and Biotechnology (KRIBB), Cheongju 28199, Korea, [4]Department of Functional Genomics, KRIBB School of Bioscience, Korea University of Science and Technology, Daejeon 34113, Korea, [5]Department of Microbiology, College of Natural Sciences, Pusan National University, Busan 46241, Korea, [6]Department of Biological Sciences, College of Natural Sciences, Pusan National University, Busan 46241, Korea
*Correspondence: khs307@pusan.ac.kr
https://doi.org/10.14348/molcells.2022.2158
www.molcells.org

MicroRNAs (miRNAs) are a class of small non-coding RNAs that regulate the expression of target messenger RNA (mRNA) complementary to the 3' untranslated region (UTR) at the post-transcriptional level. Hsa-miR-422a, which is commonly known as miRNA derived from transposable element (MDTE), was derived from short interspersed nuclear element (SINE). Through expression analysis, hsa-miR-422a was found to be highly expressed in both the small intestine and liver of crab-eating monkey. AT-Rich Interaction Domain 5 B (*ARID5B*) was selected as the target gene of hsa-miR-422a, which has two binding sites in both the exon and 3'UTR of *ARID5B*. To identify the interaction between hsa-miR-422a and *ARID5B*, a dual luciferase assay was conducted in HepG2 cell line. The luciferase activity of cells treated with the hsa-miR-422a mimic was upregulated and inversely downregulated when both the hsa-miR-422a mimic and inhibitor were administered. Nuclear factor erythroid-2 (NF-E2) was selected as the core transcription factor (TF) via feed forward loop analysis. The luciferase expression was downregulated when both the hsa-miR-422a mimic and siRNA of NF-E2 were treated, compared to the treatment of the hsa-miR-422a mimic alone. The present study suggests that hsa-miR-422a derived from SINE could bind to the exon region as well as the 3'UTR of *ARID5B*. Additionally, hsa-miR-422a was found to share binding sites in *ARID5B* with several TFs, including NF-E2. The hsa-miR-422a might thus interact with TF to regulate the expression of *ARID5B*, as demonstrated experimentally. Altogether, hsa-miR-422a acts as a super enhancer miRNA of *ARID5B* by collaborating with TF and NF-E2.

Keywords: crab-eating monkey, microRNA-422a, nuclear factor erythroid-2, short interspersed nuclear element, transposable element

INTRODUCTION

MicroRNAs (miRNAs) are 19-25 nucleotides (nt), endogenous small non-coding RNAs that are highly conserved across species, from plants to metazoan animals (Han et al., 2020; Jones-Rhoades and Bartel, 2004; Kahraman et al., 2018).

Received 17 June, 2021; revised 13 December, 2021; accepted 27 December, 2021; published online 20 April, 2022

eISSN: 0219-1032

Numerous miRNAs play a crucial role in several genetic processes, such as cell differentiation, proliferation, apoptosis, oncogenesis, and development (Cheng et al., 2005; Hwang and Mendell, 2006; Loginov et al., 2015; Neilson et al., 2007; Shivdasani, 2006). In fundamental research and reviews, the expression of numerous miRNAs has been found to be tissue- or developmental stage-specific, and changes in their expression are often detected in various pathological diseases (Ambros, 2004; Dalal and Kwon, 2010; Kahraman et al., 2018; Wienholds and Plasterk, 2005). The 5'-proximal seed region of miRNA (positions 2-8), which is approximately 6 nt sequences, binds to the 5' untranslated region (UTR) and coding region, as well as the 3'UTR of the target messenger RNA (mRNA) in the cytoplasm (Baskerville and Bartel, 2005; Forman and Coller, 2010; Lytle et al., 2007). The interaction between most miRNAs and their target genes inhibits the expression of target genes by inducing translational repression and mRNA degradation at the post-transcriptional level (Bhattacharyya et al., 2006; Djuranovic et al., 2012). However, recent studies have shown that some miRNAs are also involved in upregulating gene transcription by targeting promoter elements of the target DNA sequences, a phenomenon called RNA activation (RNAa) (Jiao and Slack, 2014; Majid et al., 2010; Matsui et al., 2013; Turner et al., 2014). In other reports, specific miRNAs were found to enhance target gene expression by correlating with other factors, including transcription factors (TFs) (Suzuki et al., 2017; Xiao et al., 2017).

MiRNAs have several genomic origins, such as intergenic regions, introns, and exons; however, specific miRNAs originate from transposable elements (TEs) (Piriyapongsa and Jordan, 2007; Yuan et al., 2010). TEs, also known as transposons, are DNA sequences that can change their position to other regions of the genome (Sun et al., 2018). TEs account for more than 50% of the human genome and are concerned with phenotypic changes and the provision of alternative promoters and enhancers by inducing intra- or inter-chromosomal rearrangements, such as insertion and deletion (INDEL) (Bailey et al., 2003; Payer and Burns, 2019). These types of INDEL events have been linked to several diseases in numerous animals, including primates. Based on the mechanisms of transposition, TEs are divided into two classes (class 1, class 2) that are activated through 'copy-and-paste' and 'cut-and-paste', respectively. Short interspersed nuclear elements (SINEs) belong to class I transposons, and the SINE-VNTR-Alus (SVA) and *Alu* elements are representatives of this class. The RNA intermediate of SINE is reverse-transcribed into complementary DNA (cDNA), and then integrated into different locations in the genome through a copy-and-paste mechanism (Bourque et al., 2018; Ullu and Tschudi, 1984). *Alu*, which is approximately 300 bp in length, is the most proliferative retrotransposon in primates, accounting for approximately 11% of the human genome (Ahl et al., 2015; Dewannieux et al., 2003). MiRNAs derived from transposable elements (MDTEs) bind to several parts of the target gene to upregulate or downregulate gene expression (He et al., 2018; Liang et al., 2016; Zou et al., 2018). One of the SINE-derived miRNAs, hsa-miR-422a, is known to play a crucial role in cancer biology as an effective tumor suppressor (Bonnin et al., 2016; Molina-Pinelo et al., 2014; Wang et al., 2017).

TFs are also important regulators of gene expression as they bind to the target DNA to modulate its transcriptional processes (Baniwal et al., 2007; Batlle et al., 2000; Coste et al., 2004; Fischer et al., 2014). Various scientific reports have shown that TFs and miRNAs can regulate each other and co-affect the same target gene by forming a feed forward loop (FFL), which is composed of two input elements and one of the other factors regulated together by input elements. Each of the three interacting factors in the FFL can either activate or repress the expression of the target gene (Wu et al., 2015; Zhang et al., 2015a; Zhou et al., 2007). Several findings suggest that TE could create genetic regulators of target genes, including TFs and miRNAs, and their interaction could affect the expression of target genes (Arora et al., 2013; Becker et al., 1993; Lee et al., 2020b; Markljung et al., 2009; Piriyapongsa et al., 2007). The present study focused on the interaction between hsa-miR-422a and its target gene, *ARID5B*. DNA sequence of *ARID5B* could provide numerous transcription factor binding sites (TFBSs), including nuclear factor erythroid-2 (NF-E2), which shares binding sequence with hsa-miR-422a. In this study, the correlation among hsa-miR-422a, *ARID5B* and NF-E2 could induce the super enhancer activity of hsa-miR-422a as a regulator of gene expression.

MATERIALS AND METHODS

Ethical statement

Experiments with Crab-eating monkey were performed in accordance with guidelines and regulation approved by Korea Research Institute of Bioscience & Biotechnology (KRIBB-AEC-15046).

Total RNA extraction of crab-eating monkey tissue samples

The tissue samples (cerebellum, cerebrum, heart, lung, liver, kidney, spleen, stomach, small intestine, colon, pancreas, bladder, and spinal cord) of crab-eating monkeys (*Macaca fascicularis*) were provided by the National Primate Research Center, Korea Research Institute of Bioscience and Biotechnology (KRIBB). Total RNA extraction from 13 tissue samples was performed using Hybrid-R™ (GeneAll, Korea), according to the manufacturer's instructions. The concentration and purity of the total RNA samples were measured using an ND-1000 UV-Vis spectrophotometer (NanoDrop Technologies, USA). To verify the integrity of the total RNA, 18s and 28s RNA bands were confirmed by gel electrophoresis.

Bioinformatic analyses of hsa-miR-422a and its target gene, *ARID5B*

The mature sequences of miR-422a of several species were obtained from miRbase v22.1 (http://www.mirbase.org) and the TE associated with hsa-miR-422a was examined using the UCSC Genome Browser (http://genome.ucsc.edu). Common target gene candidates related to hsa-miR-422a were identified from the following miRNA target prediction programs: miRDB (http://www.mirdb.org/), miRWalk3.0 (http://mirwalk.umm.uni-heidelberg.de), and DIANA-microT-CDS

(http://www.microrna.gr/microT-CDS). GO analysis was used to detect the most feasible target gene using the PANTHER classification system (http://www.pantherdb.org/). The sequences of hsa-miR-422a and the respective target regions of *ARID5B* were aligned using the program, BioEdit (https://bioedit.software.informer.com/7.2/), to confirm whether the seed region of hsa-miR-422a binds to each target region, exon, and 3'UTR in *ARID5B*. BiBiServ RNAhybrid (https://bibiserv.cebitec.uni-bielefeld.de/rnahybrid) was used to examine the interactive structures and minimum free energy (MFE) values, which predict the binding affinity of hsa-miR-422a to its binding sites in the target gene, *ARID5B*. Primers for each target site were designed using Primer3 v. 4.1, (http://primer3.ut.ee/) (Table 1).

qRT-PCR amplification for the expression analysis

Total RNA samples extracted from the tissues of crab-eating monkeys were quantified as 500 ng. To synthesize cDNA required for miRNA analysis, the HB miR Multi Assay Kit™ system I (HeimBiotek, Korea) was employed in accordance with the manufacturer's suggestions with a thermal cycler (Eppendorf, Germany) operated at 37°C for 60 min, followed by incubation at 95°C for 5 min and then holding at 4°C. HB_I Real-Time PCR Master Mix Kit (HeimBiotek) was used for quantitative real-time polymerase chain reaction (qRT-PCR) in compliance with the manufacturer's instructions, on a Rotor-Gene Q system (Qiagen, Germany) under the following conditions: initialization step at 95°C for 2 min, followed by 45 thermal cycles of 95°C for 5 s, 55°C for 10 s, and 72°C for 15 s; the standard melting conditions of the ramp ranged from 55°C to 99°C with a 1°C increase at each step. The small nuclear RNA (snRNA), U6, was used as the reference for the miRNA expression analysis. All samples were amplified in triplicate, and the relative expression data were examined using the 2-ΔCt method: ΔCt = Ct(hsa-miR-422a) − Ct(U6). The mean ± SD of the results is presented on a bar graph.

Cell culture and dual luciferase reporter assay

HepG2 (liver cancer cell line) and HUTU80 (small intestine cancer cell line) were cultured at 37°C in a 5% (v/v) CO_2 incubator in Dulbecco's modified Eagle's medium (DMEM) (Gibco, USA) containing 10% (v/v) heat-inactivated fetal bovine serum (FBS) (Gibco) and 1% (v/v) antibiotic-antimycotic (Gibco). HepG2 cells were seeded at a density of 1 × 10^5 cells/well in a 24-well plate at 80%-85% confluence and incubated for 24 h at 37°C in a 5% (v/v) CO_2 incubator. Thereafter, the cells were transfected with each psi-CHECK2 vector cloned with different binding regions of *ARID5B*, hsa-miR-422a mimic, and the inhibitor. The negative control mimic is composed of scrambled miRNAs. Hsa-miR-422a mimic is synthesized double-stranded RNAs oligonucleotide and hsa-miR-422a inhibitor is a single-stranded synthetic inhibitor which bind to complementary target miRNA. Each psi-CHECK2 vector, quantified as 500 ng, and the hsa-miR-422a mimic and inhibitor, quantified as 100 pM, were used for co-transfection using jetPRIME® (Polyplus, France), according to the manufacturer's guidelines. 1X passive buffer (Promega, USA) was used for cell lysis following 24 h of incubation, according to the manufacturer's protocol. After more than 1 day (24 h) of incubation at 80°C in a deep freezer, Firefly and Renilla luciferase activities were measured using the Dual-Luciferase® Reporter Assay System (Promega), according to the manufacturer's instructions. Each experiment was performed in triplicate, and the mean ± SD of the results is presented in a bar graph. Student's *t*-test was conducted to determine the statistical significance of the results (∗$P < 0.05$) (Excel 2016; Microsoft, USA).

Analysis of the TFBSs and siRNA treatment

TRANSFAC v8.0 (http://www.gene-regulation.com) was employed to identify the potential TFBSs on the exon and the 3'UTR regions of *ARID5B*. The threshold values and core match representing the quality of the match between the core sequences of a matrix, and the matrix match indicating the quality of the match between a matrix and a random part of the input sequence, were set to greater than 0.95 and 0.94, respectively. The FFL tool (http://bioinfo.life.hust.edu.cn/FFLtool/) was employed to reveal the core interactions among miRNAs, their target genes, and TFs. The NF-E2 siRNAs (Bioneer, Korea) and siRNA positive and negative control (Bioneer) were quantitated to 100 pM for the co-transfection of the *ARID5B*-EXON2 plasmid vector and hsa-miR-422a in HepG2 (liver cancer cell line) and HUTU80 (small intestine cancer cell line) cells. NF-E2 siRNA are composed of two sequences (5'-AGCUCCAUACCUUGGACCU-3' and 5'-AGGUCCAAGGUAUGGAGCU-3'). The siRNA positive controls

Table 1. The list of primer information on *ARID5B*

Primer	Sequence	Primer size (bp)	Product size (bp)	Details
ARID5B E1 (ARID5B:EXON1)	F: AACCAGAATGAGACGGAGGA	20	220	7mer binding site in exon region
	R: AGTAGAGCAGGGGCGTGTAA	20		
ARID5B E2 (ARID5B:EXON2)	F: GTTCCAGTTTGTCCCAGACC	20	199	6mer binding site in back side of exon region
	R: GGGTTAAGGTGATGCTTGGA	20		
ARID5B U1 (ARID5B:UTR1)	F: TGGAATATGGGGCATTTGTT	20	227	7mer in front of 3'UTR region
	R: ACTGCTTCTGTTGGGAATGC	20		
ARID5B U2 (ARID5B:UTR2)	F: AATGAGTTTGCCCTGGTGAG	20	108	8mer in back side of 3'UTR region
	R: ACCATGAGGAGACAGGCAGA	20		
GAPDH	F: GAAATCCCATCACCATCTTCCAGG	24	120	The reference gene
	R: GAGCCCCAGCCTTCTCCATG	20		

Each primer was designed based on the binding site number, location, and the length of hsa−miR−422a in *ARID5B*.

(Bioneer; Cat. No. SP-3001) were used to optimize condition about siRNA delivery and recheck high delivery level of siRNA. It is a validated siRNA known to attain high knockdown level, typically for housekeeping or a constitutively expressed gene, including GAPDH and luciferase. The siRNA negative controls (Bioneer; Cat. No. SN-1001) were used to check efficiency of transfection and determine the non-specific effects of siRNA delivery. It also known as non-targeting siRNAs that provides information of a baseline to compare to siRNA-treated groups, and contain sequences with low homology to all known human, mouse and rat genes. Using the Dual-Luciferase® Reporter Assay System (Promega), Firefly and Renilla luciferase activities were determined in accordance with the manufacturer's instructions. Each experiment was performed in triplicate, and the mean ± SD is presented in a bar graph. Student's *t*-test was conducted to determine the statistical significance of the results ($*P < 0.05$).

Relative expression analysis in HepG2 cell treated with hsa-miR-422a mimic and siRNA, NF-E2

For the expression analysis, HepG2 cells were seeded at a density of 8×10^5 cells/well in a 6-well plate at 80%-85% confluence and incubated for 24 h at 37°C in a 5% (v/v) CO_2 incubator. Thereafter, the cells were transfected with each psi-CHECK2 vector cloned with different binding regions of *ARID5B*, hsa-miR-422a mimic, and the inhibitor. Each psi-CHECK2 vector, quantified as 500 ng, and the hsa-miR-422a mimic, miRNA negative control, NF-E2 siRNA, siRNA positive control and negative control quantified as 100 pM, were used for co-transfection using jetPRIME®, according to the manufacturer's instructions. Total RNA extraction in HepG2 cell from each well was performed using Hybrid-R™ (GeneAll), along with the manufacturer's protocol. Total RNA samples isolated from the each well were calculated as 500 ng. PrimeScript RT Reagent Kit with gDNA Eraser (TaKaRa, Japan) was used for preparation of cDNA in expression analysis of *ARID5B* E2 region under the manufacturer's instructions. cDNA samples were used with the SYBR Green Q-PCR Master Mix with High Rox (SmartGene, Korea) for qRT-PCR, in accordance with manufacturer's protocol in a Rotor-Gene Q system (Qiagen) at conditions; initialization step at 95°C for 2 min, followed by 40 thermal cycles of 95°C for 5 s, 60°C for 25 s and 72°C for 15 s; standard melting conditions with 90 s at 55°C and the ramp ranged from 55°C to 99°C, with a 1°C rise at each step. Glyceraldehyde 3-phosphate dehydrogenase (*GAPDH*) was used as the reference gene for the normalization of relative expression analysis for *ARID5B*. All samples were amplified in triplicates, and the relative expression data was examined according to the 2-ΔCt method, which is ΔCt = Ct(*ARID5B*) − Ct(*GAPDH*). The mean ± SD plotted on bars in the graphs.

RESULTS

Bioinformatic and relative expression analyses of hsa-miR-422a in crab-eating monkey

The evolutionary conservation pattern and their genetic location were examined in chimpanzee, monkey, cow, dog, chicken, rat, mice, hamster, frog, and fish using the UCSC (University of California, Santa Cruz) genome browser and ECR (Evolutionary Conserved Regions) browser. Based on the results, hsa-miR-422a is derived from the transposon, SINE, and is located in the intergenic region. Hsa-miR-422a was also observed to be highly conserved in primates, including chimpanzee and monkey, and partially conserved in cow and dog (Fig. 1). Moreover, seed region of miR-422a is fully preserved in various primates, including human, chimpanzee, orangutan and rhesus monkey (Supplementary Fig. S1).

For the relative expression analysis of hsa-miR-422a, qRT-PCR was conducted using eight tissues, including brain, heart, lung, liver, kidney, spleen, stomach, small intestine, testis (male only), and bladder (female only) of male and female crab-eating monkeys. High relative expression of hsa-miR-422a was observed in the liver and small intestine of both male (Fig. 2A) and female (Fig. 2B) crab-eating monkeys.

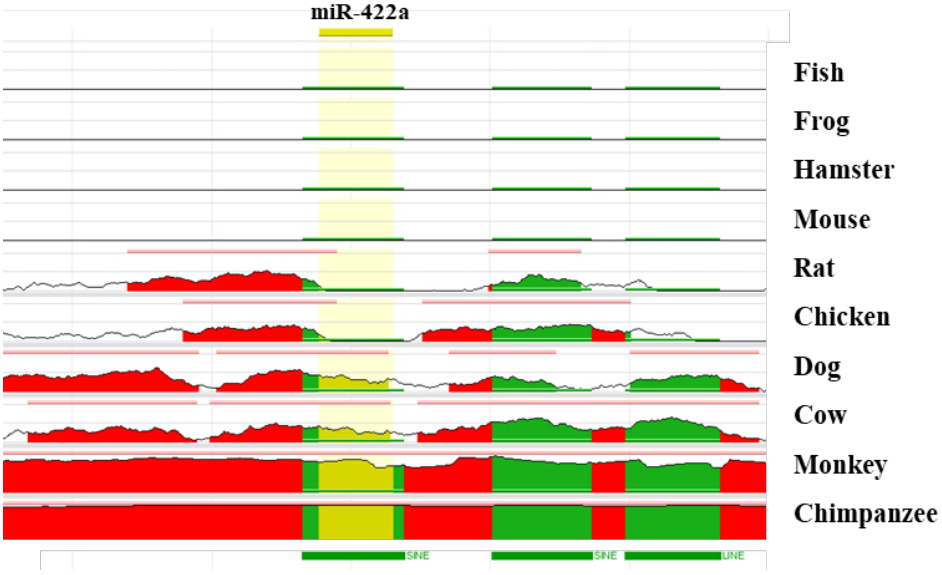

Fig. 1. Evolutionary conservation pattern of hsa-miR-422a derived from SINEs. The ECR browser revealed the evolutionary conservation in various species. Each color indicates miRNA (yellow), transposon/simple repeat (green), and intergenic region (red). Hsa-miR-422a, which originated from SINE, was highly conserved in primates and partially conserved in dog and cow.

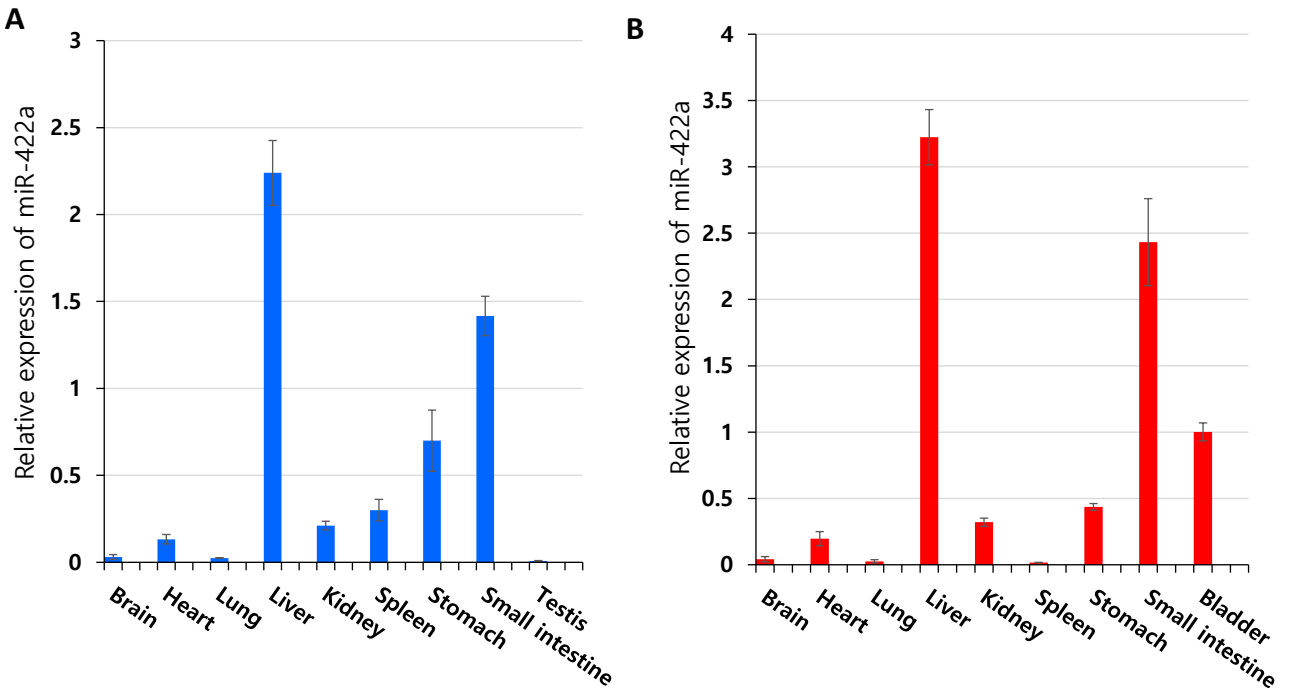

Fig. 2. Relative expression analysis of hsa-miR-422a in tissue samples from crab eating monkeys (*M. fascicularis*). (A) Relative expression of hsa-miR-422a in the male tissue samples from crab eating monkeys. (B) Relative expression of hsa-miR-422a in the female tissue samples from crab eating monkeys. Hsa-miR-422a was highly expressed in the liver and small intestine of male and female crab-eating monkeys. The relative expression of hsa-miR-422a was normalized to that of U6, which is a small nuclear RNA used as a reference RNA. The mean ± SD of triplicate measurements is presented in the bar graphs.

Bioinformatic analyses of the target gene of hsa-miR-422a in crab-eating monkey

The common target gene candidates of hsa-miR-422a were predicted using three databases: miRDB, miRWalk, and DIANA. miRDB predicted 309, miRWalk predicted 15,069, and DIANA predicted 6,343 target gene candidates separately. The common target gene candidates (216) shared by all three databases are presented in a Venn diagram (Fig. 3A). To select the crucial target gene, gene ontology (GO) analysis was conducted using the Protein ANalysis THrough Evolutionary Relationships (PANTHER) database. Thereafter, 40 genes linked with the regulation of cellular processes were categorized. Under this category, 17 genes linked with the regulation of cellular metabolic processes were identified (Fig. 3B). A list of 7 target gene candidates is presented in Fig. 3C in the order of the largest total binding sites of hsa-miR-422a among 17 genes. Among 7 candidates, AT-rich interactive domain-containing protein 5 B (*ARID5B*) was selected as the final target gene, which plays an important role in cell growth, differentiation of B-lymphocyte progenitors, and liver development. Moreover, *ARID5B* has several binding sites not only 3'UTR but also exon region. Hence, further analyses were conducted to investigate the correlation between hsa-miR-422a and various binding sites, including 3'UTR and exon region.

Bioinformatic analysis of the target gene, *ARID5B*

The mature sequence of hsa-miR-422a (5'-ACUGGACUUAGGGUCAGAAGGC-3') was downloaded from the miRBase database and aligned with the genomic sequence of the target gene, *ARID5B*, which was obtained from the UCSC genome browser. The seed region of hsa-miR-422a (5'-CUGGACU-3') binds to two different sites of the exon and the 3'UTR of *ARID5B*. The primers used in the experiments are listed in Table 1. Each primer was designed based on the binding site of hsa-miR-422a. Of the two primers that bind to the exon region, the front side primer, ARID5B E1, contains 7mer binding sites while the back side primer, ARID5B E2, contains 6mer binding sites. The primer that binds to the front of the 3'UTR, ARID5B U1, has a 7mer binding site while the back side binding primer, ARID5B U2, has 8mer binding sites. For the binding affinity analysis, the target gene sequence, including each binding site and mature sequence of hsa-miR-422a, was hybridized using the BiBiServ RNAhybrid program. For the MFE value, the larger the negative absolute value, the higher the bonding strength. The MFE value between hsa-miR-422a and the front exon region of *ARID5B* was −25.0 kcal/mol (Fig. 4A), and that of the back exon region was −23.9 kcal/mol (Fig. 4B). The MFE value between hsa-miR-422a and the front of the 3'UTR region was −16.6 kcal/mol (Fig. 4C) while that of the back 3'UTR region was −25.9 kcal/mol (Fig. 4D). These results demonstrate that hsa-miR-422a is tightly bound to *ARID5B* at each binding site.

Luciferase assay of hsa-miR-422a and *ARID5B*

Co-transfection was conducted to assess the relationship

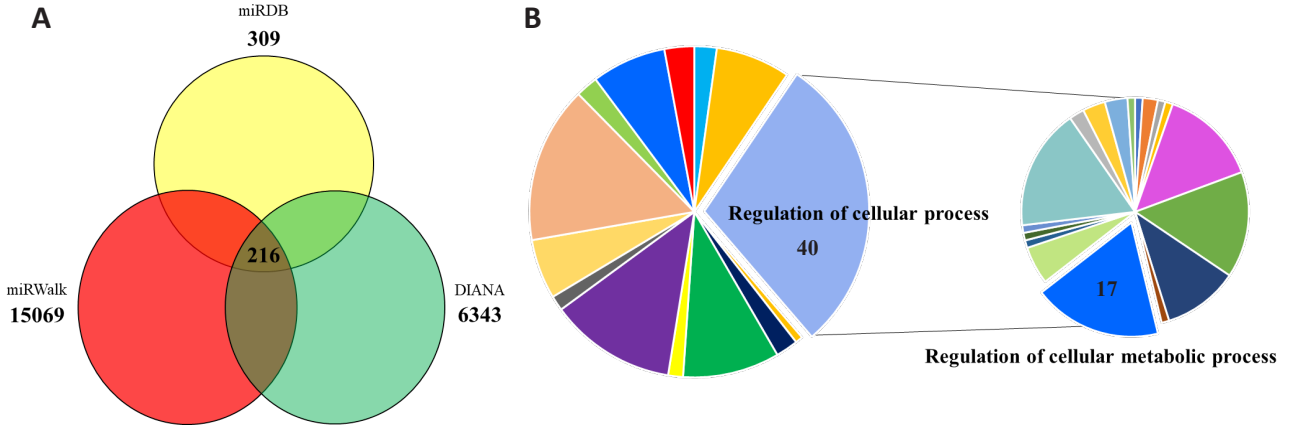

C

Gene name	Gene symbol	Total number of binding sites	Details
E2F Transcription Factor 2	E2F2	5	General transcription factor
AT-rich interactive domain-containing protein 5B	**ARID5B**	**4**	**Transcription cofactor**
Forkhead box protein I2	FOXI2	3	Winged helix/forkhead transcription factor
Probable histone-lysine N-methyltransferase PRDM7	PRDM7	3	C2H2 zinc finger transcription factor
Neuronal PAS domain-containing protein 4	NPAS4	2	Basic helix-loop-helix transcription factor
TNF receptor-associated factor 6	TRAF6	2	Scaffold/adaptor protein
Zinc Finger Protein, FOG Family Member 2	ZFPM2	1	Transcription cofactor

Fig. 3. The common target gene candidates and the results of GO analysis. (A) Venn diagram of the common predicted target genes of hsa-miR-422a based on target gene prediction programs, such as miRDB, miRwalk, and DIANA. (B) The ratio of the target gene candidates relative to the regulation of cellular process and cellular metabolic process by GO analysis for the selection of the hsa-miR-422a target gene. (C) A list of the target gene candidates that function as regulators of the cellular metabolic process, in the order of the hsa-miR-422a that binds the most to the target gene. The selected target gene, *ARID5B*, is indicated in bold.

between hsa-miR-422a and the four different binding sites of *ARID5B*. The HepG2 cell line, derived from hepatocellular carcinoma (HCC) (liver cancer), was used for co-transfection. Enhanced expression with the hsa-miR-422a mimic by approximately 1.5- to 2-fold that of the control was found in the HepG2 cell line transfected with each vector, including the ARID5B E1, ARID5B E2, ARID5B U1, and ARID5B U2 regions (Fig. 5). As shown in Figs. 5A and 5B, compared to the miRNA control, expression with the hsa-miR-422a mimic was substantially upregulated by 50% and 56.1% in the ARID5B E1 and ARID5B E2 regions, respectively. Similarly, Figs. 5C and 5D revealed that expression with the hsa-miR-422a mimic was enhanced by 59% and 86% in the ARID5B U1 and ARID5B U2 regions, respectively. When each transfected HepG2 cell line was treated with both the hsa-miR-422a mimic and inhibitor, luciferase expression was found to decrease to the level of the control at all four sites. Such findings suggest that hsa-miR-422a could provide the possibility of enhancer activity of HepG2 cells.

Prediction of the TFBSs in target gene, *ARID5B*

We performed an analysis of TFBSs under the assumption that hsa-miR-422a would interact with several TFs to show enhancer activity. The TRANSFAC v8.0 program was used to predict TFBSs in the whole genomic sequence of *ARID5B*. Among the TFs binding to each primer region, TFs whose core and matrix matches greater than 0.95 and 0.94 were respectively selected (Table 2). The following TFs were analyzed in each primer region: CREB, CREBATF, TCF-4, Lhx3, and Nkx2-5 (ARID5B E1); Hand1:E47, NF-E2, HIF-1, and AP-1 (ARID5B E2); Gfi-1, Sox-5, Sox-9, and Ik-1 (ARID5B U1); and Ik-1 and Nkx2-5 (ARID5B U2). To select the key TFs that have a distinctive correlation with hsa-miR-422a and *ARID5B*, an FFL analysis was carried out using the FFL tool. Among the TFs mentioned above, only NF-E2 formed a core FFL with hsa-miR-422a and *ARID5B* (Fig. 6). Such finding suggests that NF-E2 is an important factor related to the interaction between hsa-miR-422a and *ARID5B*.

The correlation between NF-E2 and hsa-miR-422a in the exon region of *ARID5B*

To verify the role of NF-E2 in the enhanced expression of *ARID5B*, a luciferase assay was conducted using HepG2 (Fig. 7A) and HUTU80 (Fig. 7B) cell lines originating from cancers of the liver, lung, and small intestine, respectively. When the hsa-miR-422a mimic was treated, the same increase in lucif-

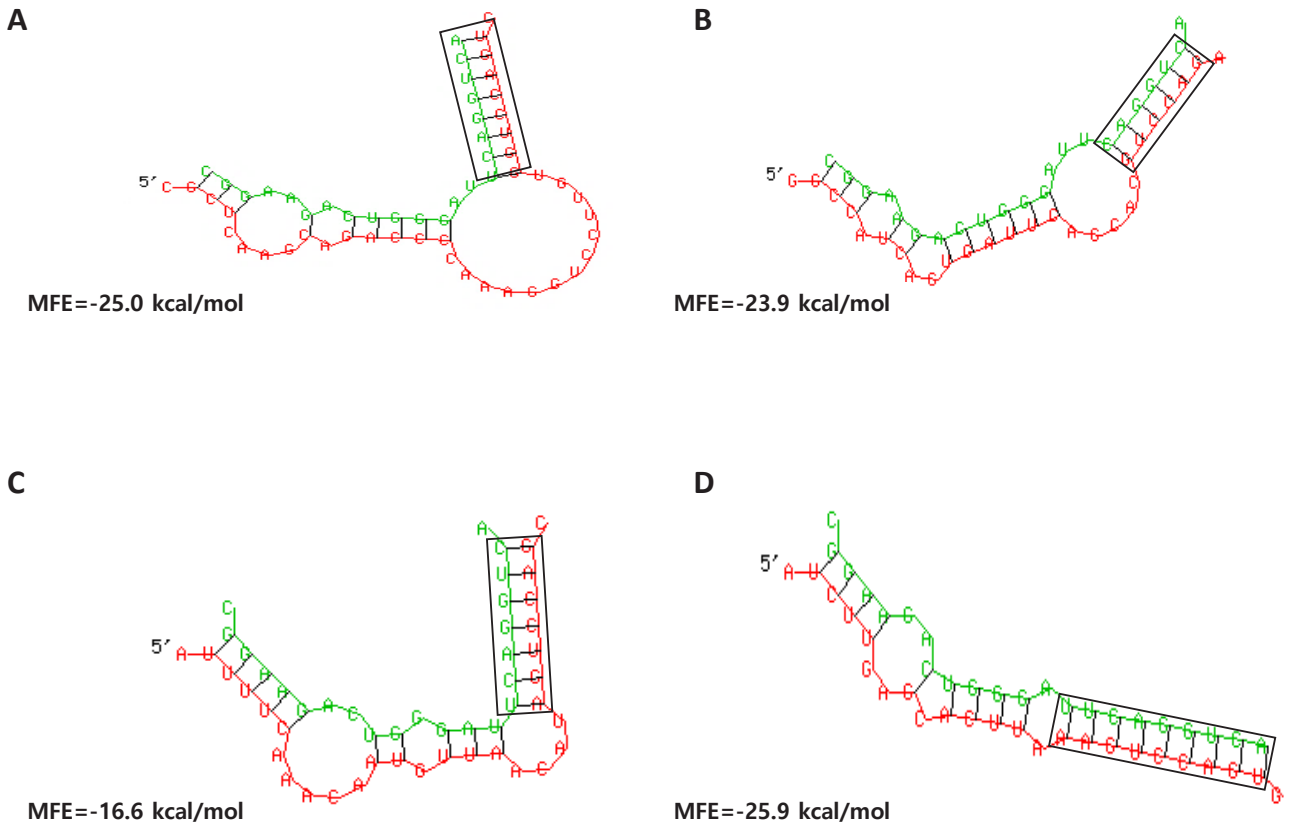

Fig. 4. RNA hybridization between hsa-miR-422a and the binding sites of *ARID5B*. The seed region of hsa-miR-422a and the binding sites of *ARID5B* are represented by black squares. (A) Results of RNA hybridization between hsa-miR-422a and ARID5B E1. The minimum free energy (MFE) value between hsa-miR-422a and ARID5B E1 was -25.0 kcal/mol. (B) Results of RNA hybridization between hsa-miR-422a and ARID5B E2. The MFE value between hsa-miR-422a and ARID5B E2 was -23.9 kcal/mol. (C) Results of RNA hybridization between hsa-miR-422a and ARID5B U1. The MFE value between hsa-miR-422a and ARID5B U1 was -16.6 kcal/mol. (D) Results of RNA hybridization between hsa-miR-422a and ARID5B U2. The MFE value between miR-422a and ARID5B U2 was -25.9 kcal/mol.

erase expression was observed in all two cell lines in comparison to the control. As shown in Fig. 7, the expression of the hsa-miR-422a mimic was substantially upregulated by 60% and 86% compared to the miRNA control in the HepG2 and HUTU80 cell lines, respectively. Inversely, luciferase expression in the ARID5B E2 region was downregulated in all two cell lines when both the hsa-miR-422a mimic and NF-E2 siRNA were injected. When each of the siRNA positive and negative control was treated with hsa-miR-422a mimic, the expression level of luciferase activity was similar to when hsa-miR-422a mimic was treated alone in the HepG2 and HUTU80 cell lines. In order to reveal whether the expression of *ARID5B* is efficiently affected by miRNA and TF, the expression level of *ARID5B* extracted from HepG2 cell, which is transfected with hsa-miR-422a mimic and NF-E2 siRNA, was checked through qRT-PCR (Supplementary Fig. S2). Consequently, *ARID5B* expression increased when hsa-miR-422a mimic was given only, and decreased when NF-E2 siRNA was simultaneously treated with hsa-miR-422a mimic. Unlike when NF-E2 siRNA is injected with hsa-miR-422a mimic, the expression of ARID5B does not change significantly after hsa-miR-422a mimic and control siRNAs (negative control or positive control) are treated together. Such finding suggests that the interaction between NF-E2 and hsa-miR-422a could promote the enhanced expression of *ARID5B*. The overall results of the experimental and bioinformatic analyses and predicted regulation model among hsa-miR-422a, TFs and ARID5B are summarized and shown as schematic illustration in Fig. 8.

DISCUSSION

Previous studies have revealed that small RNAs derived from TEs are involved in important biological processes and in several diseases, such as early development, genome dosage response, neuronal death, and several cancer types (Borges et al., 2018; Burns, 2017; Clayton et al., 2016; Lee et al., 2020a; Ohnishi et al., 2012; Sun et al., 2018). In particular, hsa-miR-422a derived from SINE is known as a tumor suppressor miRNA in several cancer types, including lung cancer, glioblastoma, colorectal cancer, osteosarcoma, and breast cancer, due to its regulation of cancer-related target genes (Wang et al., 2018; Wei et al., 2017; Wu et al., 2017; Zhang et al., 2018a; Zou et al., 2018). Hsa-miR-422a is conserved in mammals, especially primates (Fig. 1). Considering the reason for this result, hsa-miR-422a derived from SINE could have inherited characteristics of TE that jump to other sites

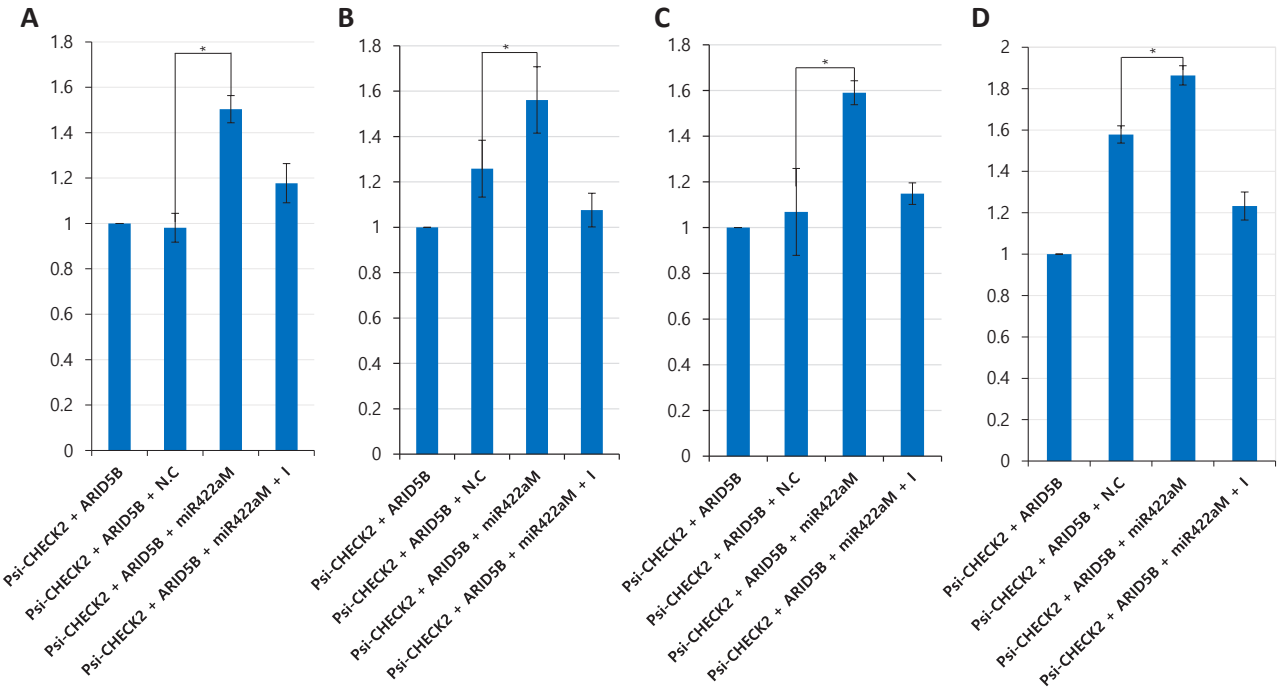

Fig. 5. Luciferase analyses of HepG2 cells co-transfected with hsa-miR-422a and each primer sites in *ARID5B*. HepG2 cells were co-transfected with two exons and two 3'UTR regions. (A) ARID5B E1. (B) ARID5B E2. (C) ARID5B U1. (D) ARID5B U2. Each binding site of *ARID5B* was cloned into the psi-CHECK2 vector and treated with hsa-miR-422a negative control (Psi-CHECK2 + ARID5B + N.C), hsa-miR-422a mimic (Psi-CHECK2 + ARID5B + miR422aM), hsa-miR-422a mimic and inhibitor (PsiCHECK2 + ARID5B + miR422aM + I). All bars are plotted based on the mean ± SD. Statistical analysis for comparisons between two groups was performed using an unpaired Student's *t*-test. Differences were considered statistically significant at $P < 0.05$. Asterisks indicate the statistical significance of the results.

Table 2. The list of TFs which bind to each primer region of *ARID5B*

Primer region	Transcription factor	Core match	Matrix match	Binding site	Direction	Sequence
ARID5B E1	CREB	1	0.947	1296	(+)	cagTGACGaca
	CREBATF	1	0.956	1298	(+)	gTGACGaca
	TCF-4	1	0.975	1363	(-)	ttCAAAGa
	Lhx3	1	0.970	1407	(+)	acTTAATtac
	Nkx2-5	1	0.977	1408	(+)	ctTAATTa
ARID5B E2	Hand1:E47	1	0.955	1589	(-)	tgtcCCAGAcccacca
	NF-E2	1	0.947	1645	(-)	gtgatTCAGCa
	HIF-1	1	0.956	1650	(-)	tcagCACGTcca
	AP-1	0.955	0.967	1645	(+)	gtgATTCAg
ARID5B U1	Gfi-1	1	0.974	5373	(-)	ttccactgcaaTGATTtcagtctg
	Sox-5	1	0.995	5431	(+)	caaACAATgt
	Sox-9	1	0.951	5429	(+)	ttcaaACAATgtta
	Ik-1	1	0.964	5557	(-)	cgcaTTCCCaaca
ARID5B U2	Ik-1	1	0.953	6365	(+)	aaatGGGAAtgag
	Nkx2-5	1	0.986	6421	(-)	CACTTaa

The TFBSs in each primer region were predicted by TRANSFAC v8.0 program, and TFs whose core and matrix matches greater than 0.95 and 0.94 were respectively selected.

of the genomic region. In studies related to transposons, each species was confirmed to have different amounts of TE in each genome, and the contribution of DNA transposons and retrotransposons to the percentage of each species of TE differs in many eukaryotic species (Feschotte and Pritham, 2007; Hirsch and Springer, 2017). To analyze the biological role of hsa-miR-422a in primates, qRT-PCR was conducted in eight organs of crab-eating monkeys. The highest expression

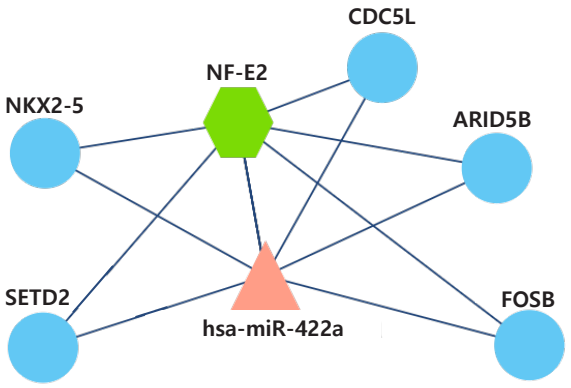

Fig. 6. FFL analysis of hsa-miR-422a, *ARID5B*, and several transcription factors. Based on FFL analysis, NF-E2 was selected as the core transcription factor and was further correlated with hsa-miR-422a and *ARID5B*. Hsa-miR-422a (expressed by red triangle) and NF-E2 (transcription factor expressed by green hexagon) were found to regulate each other and co-regulate the same target gene, *ARID5B* (target gene of hsa-miR-422a depicted by a blue circle).

of hsa-miR-422a was confirmed to be in the liver of both male and female crab-eating monkeys (Fig. 2). Several studies have revealed the relationship between hsa-miR-422a and liver-related diseases. Hsa-miR-122 and hsa-miR-422a could destabilize the mRNA of cytochrome P450 7A1 (CYP7A1), also known as cholesterol 7 alpha-hydroxylase, by inhibiting CYP7A1 expression, which plays an important role in the regulation of bile acid synthesis in the liver (Song et al., 2010). In HCC, hsa-miR-422a acts as a regulator of several factors. One study revealed that DUXAP8 could function as an oncogenic lncRNA in HCC by repressing the tumor suppressor miRNA, hsa-miR-422a, and increasing the expression of pyruvate dehydrogenase kinase 2 through an indirect pathway (Wei et al., 2020). Another study showed that the expression of hsa-miR-422a was downregulated by three target genes, forkhead box G1 (*FOXG1*), *FOXQ1*, and *FOXE1* in HCC and formed a double-negative feedback loop among hsa-miR-422a and these targets to regulate HCC development (Zhang et al., 2015b). Hsa-miR-422a is also related to the pathogenesis of liver fibrosis as it forms an miRNA-gene regulatory module with four miRNAs (miR-130b-3p, miR-148a-3p, miR-345-5p, and miR-378a-3p) and six genes (*COL6A1*, *COL6A2*,

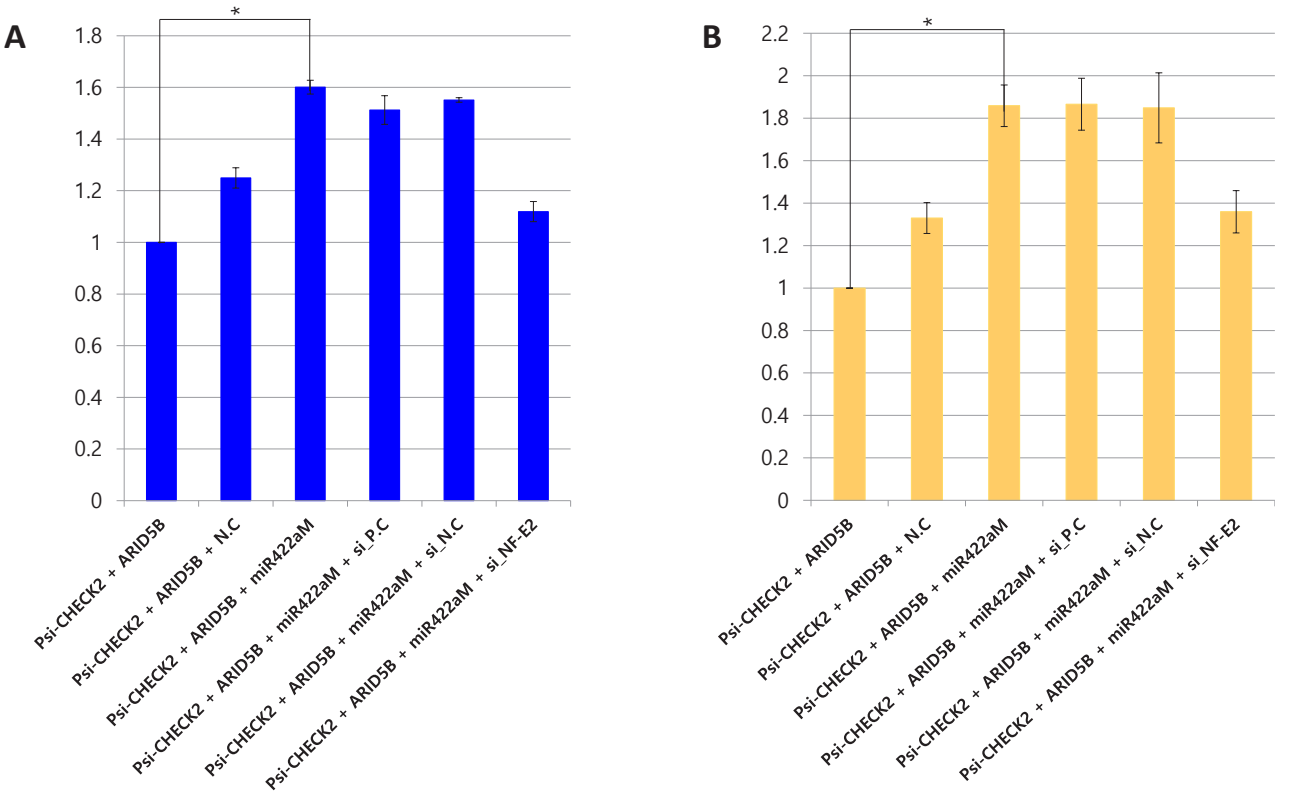

Fig. 7. Luciferase analyses of the ARID5B E2 region co-transfected with hsa-miR-422a mimic and siRNA of the transcription factor, NF-E2. (A) The result of Luciferase assay in HepG2 cells. (B) The result of Luciferase assay in HUTU80 cells. The ARID5B E2 region was cloned into the psi-CHECK2 vector and treated with hsa-miR-422a negative control (Psi-CHECK2 + ARID5B + N.C), hsa-miR-422a mimic (Psi-CHECK2 + ARID5B + miR422aM), has-miR-422a mimic, siRNA positive control (Psi-CHECK2 + ARID5B + miR422aM + si_P.C), hsa-miR-422a mimic, siRNA negative control (Psi-CHECK2 + ARID5B + miR422aM + si_N.C), and hsa-miR-422a mimic, NF-E2 siRNA (PsiCHECK2 + ARID5B + miR422aM + si_NF-E2). All bars represent the mean ± SD. Statistical analysis for comparisons between two groups was performed using an unpaired Student's *t*-test. Differences were considered statistically significant at $P < 0.05$. Asterisks indicate the statistical significance of the results.

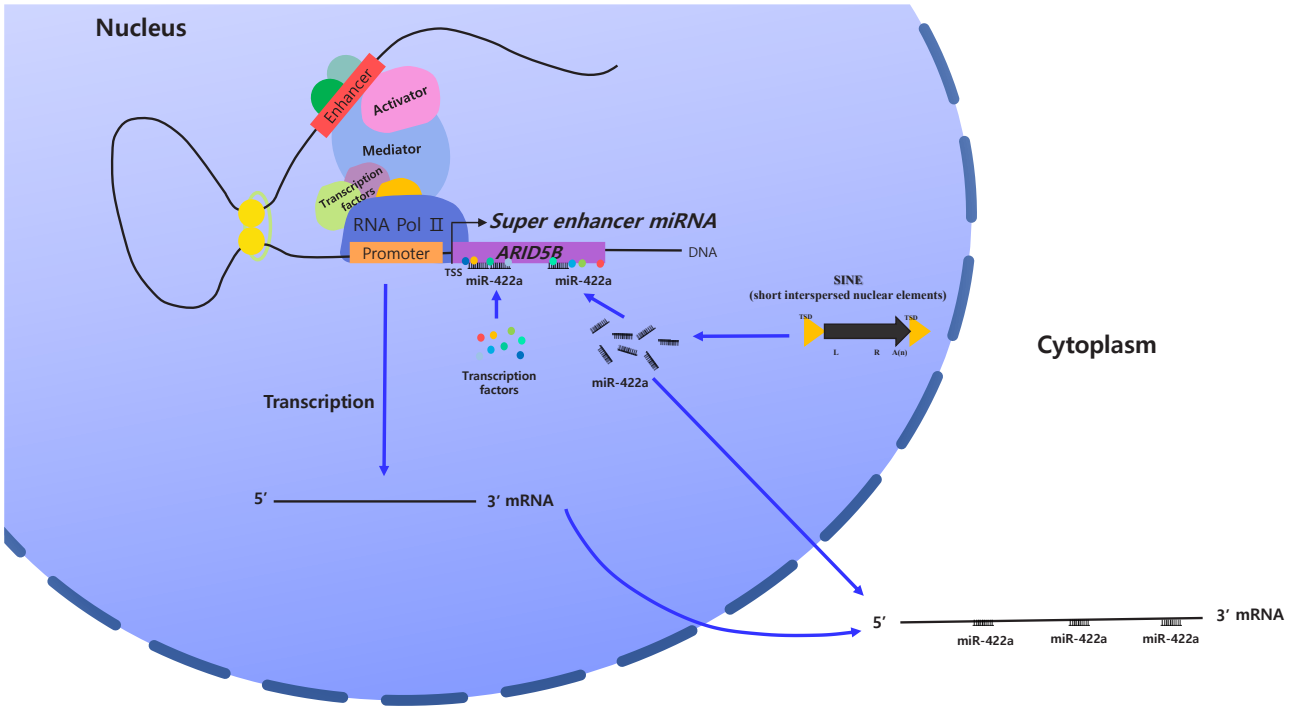

Fig. 8. Schematic illustration of *ARID5B* enhancer activity upregulated by hsa-miR-422a. Hsa-miR-422a, which is derived from SINE, bind to DNA sequences of target gene, ARID5B and interact with numerous transcription factors around binding sites of hsa-miR-422a. In addition, some hsa-miR-422a correlate with mRNA of ARID5B, and all of these interactions support overall regulation of ARID5B expression. The correlation between hsa-miR-422a and transcription factors induces up-regulated expression of ARID5B. In other words, hsa-miR-422a act as super enhancer miRNA and core regulator by regulation of transcriptional and post-transcriptional expression of ARID5B. TSS, transcription start site; TSD, tandem site duplication.

COL6A3, *PIK3R3*, *COL1A1*, and *CCND2*) (Chen et al., 2017). In nonalcoholic fatty liver disease, decreased expression of miR-139-5p, miR-30b-5p, miR-422a, and miR-146a by palmitic acid resulted in decreased liver glucose and lipid metabolism, but increased fatty acid biosynthesis (Latorre et al., 2017). Herein, we conducted several experimental and bioinformatic analyses to evaluate whether hsa-miR-422a could control various biological processes related to the liver, based on recent reports and the relative expression patterns.

ARID5B was selected as the target gene of hsa-miR-422a using various target gene prediction tools. Thereafter, the binding sites between the seed regions of hsa-miR-422a and *ARID5B* were analyzed. *ARID5B* was confirmed to have a total of four binding sites for hsa-miR-422a, two in the exon and 3'UTR. MiRNAs are usually known to interact with the 3'UTR to regulate the expression of target mRNAs and related biological processes. However, recent studies have shown that miRNAs can modulate their expression by collaborating with other sites, such as the DNA sequences, 5'UTR, intron, or exon region as well as the 3'UTR (Kumar et al., 2012; Lin et al., 2008; Zhou et al., 2009). According to experimental studies related to the 5'UTR, miR-10a and miR-346 could upregulate the translation of target mRNA and increase protein expression levels (Ørom et al., 2008; Tsai et al., 2009). Through single nucleotide polymorphism analysis in exonic regions, multiple miRNAs, including miR-671-3p and miR-657, are known to interact with the coding region of metalloproteinase and regulate its expression (Duellman et al., 2014). Likewise, miR-193b-5p affects the migration and metastasis of breast cancer, and miR-31-5p improves amyloid-beta pathology in Alzheimer's disease by regulating the coding region of the target gene, *CD44v6*, and amyloid precursor protein (APP) (Barros-Viegas et al., 2020; Hu et al., 2020). In light of these recent reports, these findings suggest that the collaboration between hsa-miR-422a and the coding regions could also affect the regulation of gene expression.

ARID5B is a well-known critical oncogenic factor that contributes to T-cell leukemogenesis in acute lymphoblastic leukemia; however, this factor is also involved in liver-related diseases. *ARID5B* is upregulated in hepatic stellate cells (HSCs) and can promote liver fibrosis by activating HSCs, which play a crucial role in liver fibrogenesis of different etiologies (He et al., 2020). Based on studies of HCC, 55% (98 of 179) of genes, including *ARID5B*, that impact liver development, had differential expression in cirrhotic or HCC samples compared to normal samples (Behnke et al., 2012). In addition, single nucleotide variants that are exclusively present in the progression to HCC are related to genes (*ARID3A*, *ARID3C*, *ARID4A*, *ARID5B*) involved in chromatin remodeling (Fujimoto et al., 2012; Guichard et al., 2012). The present experiment was conducted to determine whether hsa-miR-422a and *ARID5B* share the same regulatory interaction in the liver,

taking into account prior liver-related studies of hsa-miR-422a and *ARID5B*. To investigate the correlation between hsa-miR-422a and *ARID5B*, a luciferase assay was performed in vitro. Consequently, the expression of *ARID5B* in HepG2 cells co-transfected with psi-CHECK2 vector cloned with four binding sites of hsa-miR-422a and the hsa-miR-422a mimic was significantly increased compared to the control. The luciferase assay was also carried out to examine the coding region; however, there was no substantial difference in expression between the coding regions and the 3'UTR (Fig. 5). This upregulated result could be explained by hsa-miR-422a acting as an enhancer to increase the expression of *ARID5B*.

In most papers on miRNA, miRNAs have been reported to regulate their target genes by repression; however, several studies have shown that some miRNAs might have enhancer functions on target genes. One study revealed that miR-24-1 can stimulate gene transcription by binding to enhancer sequences and increasing the expression of the enhancer RNA, which promotes histone alteration and the enrichment of p300 and RNA Pol II (Xiao et al., 2017). Additionally, hsa-miR-205 activates the expression of tumor suppressor genes, such as interleukin (IL) 24 and IL32, by binding to specific sites of promoters at the transcriptional level (Majid et al., 2010). A few studies have also shown that MDTEs can upregulate the expression of each target gene. In a study of hsa-miR-625-3p derived from long interspersed nuclear element (LINE), a high expression level of hsa-miR-625-3p was observed in tumor tissues with papillary thyroid cancer compared to adjacent normal tissues. Further, hsa-miR-625-3p was found to stimulate the proliferation, migration, and invasion of thyroid cancer cells (SW579 and TPC-1 cells) by increasing the expression of the target gene, *AEG-1*, which activates the Wnt/β-catenin and JNK pathways (Fang et al., 2018). Additionally, hsa-miR-3681-5p originating from endogenous retroviruses leads to super enhancer activity by collaborating with the 3'UTR of SHISA7 in the A549 cell line (Lee et al., 2020b). According to previous reports, miRNA, especially MDTE such as hsa-miR-422a, has the potential to regulate target genes as super-enhancer miRNAs. We hypothesized that the enhancer activity of hsa-miR-422a on *ARID5B* expression might be related to some interaction with certain factors including TFs. Based on previous studies on miRNAs that exert enhancer activity on target genes, TFs might be involved in the enhancer relationship between miRNA and target genes by forming FFL (Brosh et al., 2008; Peng et al., 2013; Zhang et al., 2015a). Therefore, we identified the TFBSs using the TRANSFAC program to determine the TFs that collaborate with each primer site of *ARID5B* (Table 2). Among several TFs that share binding sites with hsa-miR-422a, FFL analysis predicted that NF-E2 is a key regulator of the most core regulation (Fig. 6). NF-E2 shares some of the binding sites, especially in the primer E2 region, with hsa-miR-422a. Collectively, such findings suggest that the three factors, hsa-miR-422a, NF-E2, and *ARID5B*, could co-affect the same biological function by forming FFL.

The hematopoietic TF, NF-E2, is a heterodimeric leucine zipper TF required for megakaryocyte differentiation (Andrews et al., 1993; Goerttler et al., 2005; Kacena et al., 2004). Some studies have revealed that NF-E2, which functions as an essential regulator of globin gene expression by regulating erythroid and megakaryocytic maturation, has TF activity and transcription coactivator activity (Andrews et al., 1993; Hung et al., 2001; Sawado et al., 2001). In a study of patients with myeloproliferative neoplasms, mutated and truncated NF-E2 were found to cause erythrocytosis and thrombocytosis, and increase the proliferative advantage (Jutzi et al., 2013). As hsa-miR-422a and *ARID5B* are associated with liver-related diseases, NF-E2 is also involved in liver-related pathological processes, such as hepatomegaly and extramedullary hematopoiesis induced by erythrocytosis and thrombocytosis, according to previous studies (Gregory et al., 1983; Jelkmann, 2001; Ohta et al., 2002; Spivak, 2010). A study on insulin resistance revealed that exercise performed by subjects with diet-induced obesity induces a reduction in NFE2/miR-423-5p, inversely enhancing FAM3A. Consequently, this change promotes the FAM3A ATP-Akt pathway in the liver and improves hepatic insulin sensitivity and whole-body insulin resistance (Yang et al., 2017; Zhang et al., 2018b). To verify the connection between hsa-miR-422a, *ARID5B*, and NF-E2 at the cellular level, a luciferase assay with siRNA treatment was performed. The expression of the primer E2 region in *ARID5B* was found to increase in the two cell lines (HepG2 and HUTU80) treated with the hsa-miR-422a mimic, and inversely decrease when the siRNA of NF-E2 and the hsa-miR-422a mimic were treated together (Fig. 7). The qRT-PCR was performed for examining the expression change of *ARID5B in vitro* level and the result have shown that *ARID5B* expression in hepG2 cell increased when mimic was treated only. In contrast, when NF-E2 siRNA was simultaneously treated with hsa-miR-422a mimic, ARID5B expression decreased. These experimental results suggest that hsa-miR-422a and NF-E2 could interact with each other to enhance their respective function. This enhanced expression is supported by various studies on the relationship among these TF-miRNA-target genes. OF-miR-307 acts as a super enhancer miRNA by providing binding sites with several TFs in the 3'UTR of the target gene, *mkl1*, including Sox-5, GATA-1, HNF-6, FOXO1, and HFH-3 (Lee et al., 2019). Another MDTE-related report also found that hsa-miR-625-5p derived from LINE binds to the 3'UTR of *GATAD2B* and exhibits enhancer activity supported by NF-κB in the A549 cell line (Lee et al., 2021). Consequently, such findings suggest that NF-E2 might interact with hsa-miR-422a as a super enhancer miRNA to enhance the expression of *ARID5B*.

In summary, hsa-miR-422a derived from SINE could interact with the coding regions and the 3'UTR of ARID5B in nucleus and cytoplasm. Several TFs, including NF-E2, could bind to each binding site of hsa-miR-422a in DNA sequence of ARID5B. Mainly, hsa-miR-422a could interact with DNA of ARID5B and upregulates expression of ARID5B supported by TFs in nucleus. Also, in cytoplasm, hsa-miR-422a might interact with mRNA of ARID5B, and participate in regulation of gene expression. Overall, hsa-miR-422a exerted enhancer activity to ARID5B by forming an FFL among hsa-miR-422a, TFs, and DNA sequence of ARID5B (Fig. 8). These findings suggest that hsa-miR-422a regulates the expression of *ARID5B* and NF-E2 promotes its enhancer activity by sharing binding sites with hsa-miR-422a to act as an alternative promoter and

enhancer. The correlation among hsa-miR-422a, *ARID5B*, and NF-E2 in liver-related processes should be analyzed for further functional studies.

Note: Supplementary information is available on the Molecules and Cells website (www.molcells.org).

ACKNOWLEDGMENTS

This research was supported by the National Research Foundation of Korea (NRF) funded by the Ministry of Education (NRF-2018R1D1A1B07049460).

AUTHOR CONTRIBUTIONS

W.R.K. designed and performed all experiments and wrote the manuscript. J.W.H., S.J.P., and H.E.L. provided the crab-eating monkey samples. E.G.P., J.N.K., and H.S.K. revised the manuscript. All authors have read and agreed to the final version of the manuscript.

CONFLICT OF INTEREST

The authors have no potential conflicts of interest to disclose.

ORCID

Woo Ryung Kim https://orcid.org/0000-0003-1840-4444
Eun Gyung Park https://orcid.org/0000-0002-9575-7043
Hee-Eun Lee https://orcid.org/0000-0002-7485-9083
Sang-Je Park https://orcid.org/0000-0002-3371-9092
Jae-Won Huh https://orcid.org/0000-0001-5845-939X
Jeong Nam Kim https://orcid.org/0000-0002-6825-0407
Heui-Soo Kim https://orcid.org/0000-0002-5226-6594

REFERENCES

Ahl, V., Keller, H., Schmidt, S., and Weichenrieder, O. (2015). Retrotransposition and crystal structure of an Alu RNP in the ribosome-stalling conformation. Mol. Cell *60*, 715-727.

Ambros, V. (2004). The functions of animal microRNAs. Nature *431*, 350-355.

Andrews, N.C., Erdjument-Bromage, H., Davidson, M.B., Tempst, P., and Orkin, S.H. (1993). Erythroid transcription factor NF-E2 is a haematopoietic-specific basic–leucine zipper protein. Nature *362*, 722-728.

Arora, S., Rana, R., Chhabra, A., Jaiswal, A., and Rani, V. (2013). miRNA–transcription factor interactions: a combinatorial regulation of gene expression. Mol. Genet. Genomics *288*, 77-87.

Bailey, J.A., Liu, G., and Eichler, E.E. (2003). An Alu transposition model for the origin and expansion of human segmental duplications. Am. J. Hum. Genet. *73*, 823-834.

Baniwal, S.K., Chan, K.Y., Scharf, K.D., and Nover, L. (2007). Role of heat stress transcription factor HsfA5 as specific repressor of HsfA4. J. Biol. Chem. *282*, 3605-3613.

Barros-Viegas, A.T., Carmona, V., Ferreiro, E., Guedes, J., Cardoso, A.M., Cunha, P., de Almeida, L.P., de Oliveira, C.R., de Magalhães, J.P., Peça, J., et al. (2020). miRNA-31 improves cognition and abolishes amyloid-β pathology by targeting APP and BACE1 in an animal model of Alzheimer's disease. Mol. Ther. Nucleic Acids *19*, 1219-1236.

Baskerville, S. and Bartel, D.P. (2005). Microarray profiling of microRNAs reveals frequent coexpression with neighboring miRNAs and host genes. RNA *11*, 241-247.

Batlle, E., Sancho, E., Francí, C., Domínguez, D., Monfar, M., Baulida, J., and De Herreros, A.G. (2000). The transcription factor snail is a repressor of E-cadherin gene expression in epithelial tumour cells. Nat. Cell Biol. *2*, 84-89.

Becker, K.G., Swergold, G., Ozato, K., and Thayer, R.E. (1993). Binding of the ubiquitous nuclear transcription factor YY1 to a cis regulatory sequence in the human LINE-1 transposable element. Hum. Mol. Genet. *2*, 1697-1702.

Behnke, M., Reimers, M., and Fisher, R. (2012). The expression of embryonic liver development genes in hepatitis C induced cirrhosis and hepatocellular carcinoma. Cancers (Basel) *4*, 945-968.

Bhattacharyya, S.N., Habermacher, R., Martine, U., Closs, E.I., and Filipowicz, W. (2006). Relief of microRNA-mediated translational repression in human cells subjected to stress. Cell *125*, 1111-1124.

Bonnin, N., Armandy, E., Carras, J., Ferrandon, S., Battiston-Montagne, P., Aubry, M., Guihard, S., Meyronet, D., Foy, J.P., Saintigny, P., et al. (2016). MiR-422a promotes loco-regional recurrence by targeting NT5E/CD73 in head and neck squamous cell carcinoma. Oncotarget *7*, 44023-44038.

Borges, F., Parent, J.S., van Ex, F., Wolff, P., Martínez, G., Köhler, C., and Martienssen, R.A. (2018). Transposon-derived small RNAs triggered by miR845 mediate genome dosage response in Arabidopsis. Nat. Genet. *50*, 186-192.

Bourque, G., Burns, K.H., Gehring, M., Gorbunova, V., Seluanov, A., Hammell, M., Imbeault, M., Izsvák, Z., Levin, H.L., Macfarlan, T.S., et al. (2018). Ten things you should know about transposable elements. Genome Biol. *19*, 199.

Brosh, R., Shalgi, R., Liran, A., Landan, G., Korotayev, K., Nguyen, G.H., Enerly, E., Johnsen, H., Buganim, Y., Solomon, H., et al. (2008). p53-repressed miRNAs are involved with E2F in a feed-forward loop promoting proliferation. Mol. Syst. Biol. *4*, 229.

Burns, K.H. (2017). Transposable elements in cancer. Nat. Rev. Cancer 17, 415-424.

Chen, W., Zhao, W., Yang, A., Xu, A., Wang, H., Cong, M., Liu, T., Wang, P., and You, H. (2017). Integrated analysis of microRNA and gene expression profiles reveals a functional regulatory module associated with liver fibrosis. Gene *636*, 87-95.

Cheng, A.M., Byrom, M.W., Shelton, J., and Ford, L.P. (2005). Antisense inhibition of human miRNAs and indications for an involvement of miRNA in cell growth and apoptosis. Nucleic Acids Res. *33*, 1290-1297.

Clayton, E.A., Wang, L., Rishishwar, L., Wang, J., McDonald, J.F., and Jordan, I.K. (2016). Patterns of transposable element expression and insertion in cancer. Front. Mol. Biosci. *3*, 76.

Coste, A.T., Karababa, M., Ischer, F., Bille, J., and Sanglard, D. (2004). TAC1, transcriptional activator of CDR genes, is a new transcription factor involved in the regulation of Candida albicans ABC transporters CDR1 and CDR2. Eukaryot. Cell *3*, 1639-1652.

Dalal, S.R. and Kwon, J.H. (2010). The role of microRNA in inflammatory bowel disease. Gastroenterol. Hepatol. (N.Y.) *6*, 714-722.

Dewannieux, M., Esnault, C., and Heidmann, T. (2003). LINE-mediated retrotransposition of marked Alu sequences. Nat. Genet. *35*, 41-48.

Djuranovic, S., Nahvi, A., and Green, R. (2012). miRNA-mediated gene silencing by translational repression followed by mRNA deadenylation and decay. Science *336*, 237-240.

Duellman, T., Warren, C., and Yang, J. (2014). Single nucleotide polymorphism-specific regulation of matrix metalloproteinase-9 by multiple miRNAs targeting the coding exon. Nucleic Acids Res. *42*, 5518-5531.

Fang, L., Kong, D., and Xu, W. (2018). MicroRNA-625-3p promotes the proliferation, migration and invasion of thyroid cancer cells by up-regulating astrocyte elevated gene 1. Biomed. Pharmacother. *102*, 203-211.

Feschotte, C. and Pritham, E.J. (2007). DNA transposons and the evolution of eukaryotic genomes. Annu. Rev. Genet. *41*, 331-368.

Fischer, M., Steiner, L., and Engeland, K. (2014). The transcription factor p53: not a repressor, solely an activator. Cell Cycle *13*, 3037-3058.

Forman, J.J. and Coller, H.A. (2010). The code within the code: microRNAs target coding regions. Cell Cycle *9*, 1533-1541.

Fujimoto, A., Totoki, Y., Abe, T., Boroevich, K.A., Hosoda, F., Nguyen, H.H., Aoki, M., Hosono, N., Kubo, M., Miya, F., et al. (2012). Whole-genome sequencing of liver cancers identifies etiological influences on mutation patterns and recurrent mutations in chromatin regulators. Nat. Genet. *44*, 760-764.

Goerttler, P.S., Kreutz, C., Donauer, J., Faller, D., Maiwald, T., März, E., Rumberger, B., Sparna, T., Schmitt-Gräff, A., Wilpert, J., et al. (2005). Gene expression profiling in polycythaemia vera: overexpression of transcription factor NF-E2. Br. J. Haematol. *129*, 138-150.

Gregory, P., Marsh, W.H., Cunningham, J.T., and Lee, W.M. (1983). Hepatomegaly and ascites in an elderly woman with polycythemia vera. J. Clin. Gastroenterol. *5*, 367-376.

Guichard, C., Amaddeo, G., Imbeaud, S., Ladeiro, Y., Pelletier, L., Maad, I.B., Calderaro, J., Bioulac-Sage, P., Letexier, M., Degos, F., et al. (2012). Integrated analysis of somatic mutations and focal copy-number changes identifies key genes and pathways in hepatocellular carcinoma. Nat. Genet. *44*, 694-698.

Han, X., Luan, T., Sun, Y., Yan, W., Wang, D., and Zeng, X. (2020). MicroRNA 449c mediates the generation of monocytic myeloid-derived suppressor cells by targeting STAT6. Mol. Cells *43*, 793-803.

He, L., Yuan, H., Liang, J., Hong, J., and Qu, C. (2020). Expression of hepatic stellate cell activation-related genes in HBV-, HCV-, and nonalcoholic fatty liver disease-associated fibrosis. PLoS One *15*, e0233702.

He, Z., Li, Z., Zhang, X., Yin, K., Wang, W., Xu, Z., Li, B., Zhang, L., Xu, J., Sun, G., et al. (2018). MiR-422a regulates cellular metabolism and malignancy by targeting pyruvate dehydrogenase kinase 2 in gastric cancer. Cell Death Dis. *9*, 505.

Hirsch, C.D. and Springer, N.M. (2017). Transposable element influences on gene expression in plants. Biochim. Biophys. Acta Gene Regul. Mech. *1860*, 157-165.

Hu, S., Cao, M., He, Y., Zhang, G., Liu, Y., Du, Y., Yang, C., and Gao, F. (2020). CD44v6 targeted by miR-193b-5p in the coding region modulates the migration and invasion of breast cancer cells. J. Cancer *11*, 260-271.

Hung, H.L., Kim, A.Y., Hong, W., Rakowski, C., and Blobel, G.A. (2001). Stimulation of NF-E2 DNA binding by CREB-binding protein (CBP)-mediated acetylation. J. Biol. Chem. *276*, 10715-10721.

Hwang, H. and Mendell, J. (2006). MicroRNAs in cell proliferation, cell death, and tumorigenesis. Br. J. Cancer *94*, 776-780.

Jelkmann, W. (2001). The role of the liver in the production of thrombopoietin compared with erythropoietin. Eur. J. Gastroenterol. Hepatol. *13*, 791-801.

Jiao, A.L. and Slack, F.J. (2014). RNA-mediated gene activation. Epigenetics *9*, 27-36.

Jones-Rhoades, M.W. and Bartel, D.P. (2004). Computational identification of plant microRNAs and their targets, including a stress-induced miRNA. Mol. Cell *14*, 787-799.

Jutzi, J.S., Bogeska, R., Nikoloski, G., Schmid, C.A., Seeger, T.S., Stegelmann, F., Schwemmers, S., Gründer, A., Peeken, J.C., Gothwal, M., et al. (2013). MPN patients harbor recurrent truncating mutations in transcription factor NF-E2. J. Exp. Med. *210*, 1003-1019.

Kacena, M.A., Shivdasani, R.A., Wilson, K., Xi, Y., Troiano, N., Nazarian, A., Gundberg, C.M., Bouxsein, M.L., Lorenzo, J.A., and Horowitz, M.C. (2004). Megakaryocyte-osteoblast interaction revealed in mice deficient in transcription factors GATA-1 and NF-E2. J. Bone Miner. Res. *19*, 652-660.

Kahraman, M., Röske, A., Laufer, T., Fehlmann, T., Backes, C., Kern, F., Kohlhaas, J., Schrörs, H., Saiz, A., Zabler, C., et al. (2018). MicroRNA in diagnosis and therapy monitoring of early-stage triple-negative breast cancer. Sci. Rep. *8*, 11584.

Kumar, A., Wong, A.K.L., Tizard, M.L., Moore, R.J., and Lefèvre, C. (2012). miRNA_Targets: a database for miRNA target predictions in coding and non-coding regions of mRNAs. Genomics *100*, 352-356.

Latorre, J., Moreno-Navarrete, J., Mercader, J., Sabater, M., Rovira, O., Gironès, J., Ricart, W., Fernandez-Real, J., and Ortega, F. (2017). Decreased lipid metabolism but increased FA biosynthesis are coupled with changes in liver microRNAs in obese subjects with NAFLD. Int. J. Obes. (Lond.) *41*, 620-630.

Lee, H.E., Huh, J.W., and Kim, H.S. (2020a). Bioinformatics analysis of evolution and human disease related transposable element-derived microRNAs. Life (Basel) *10*, 95.

Lee, H.E., Jo, A., Im, J., Cha, H.J., Kim, W.J., Kim, H.H., Kim, D.S., Kim, W., Yang, T.J., and Kim, H.S. (2019). Characterization of the long terminal repeat of the endogenous retrovirus-derived microRNAs in the olive flounder. Sci. Rep. *9*, 14007.

Lee, H.E., Park, S.J., Huh, J.W., Imai, H., and Kim, H.S. (2020b). Enhancer function of microRNA-3681 derived from long terminal repeats represses the activity of variable number tandem repeats in the 3'UTR of SHISA7. Mol. Cells *43*, 607-618.

Lee, H.E., Park, S.J., Huh, J.W., Imai, H., and Kim, H.S. (2021). The enhancer activity of long interspersed nuclear element derived microRNA 625 induced by NF-κB. Sci. Rep. *11*, 3139.

Liang, H., Wang, R., Jin, Y., Li, J., and Zhang, S. (2016). MiR-422a acts as a tumor suppressor in glioblastoma by targeting PIK3CA. Am. J. Cancer Res. *6*, 1695-1707.

Lin, S.L., Kim, H., and Ying, S.Y. (2008). Intron-mediated RNA interference and microRNA (miRNA). Front. Biosci. *13*, 2216-2230.

Loginov, V., Rykov, S., Fridman, M., and Braga, E. (2015). Methylation of miRNA genes and oncogenesis. Biochemistry (Mosc.) *80*, 145-162.

Lytle, J.R., Yario, T.A., and Steitz, J.A. (2007). Target mRNAs are repressed as efficiently by microRNA-binding sites in the 5′ UTR as in the 3′ UTR. Proc. Natl. Acad. Sci. U. S. A. *104*, 9667-9672.

Majid, S., Dar, A.A., Saini, S., Yamamura, S., Hirata, H., Tanaka, Y., Deng, G., and Dahiya, R. (2010). MicroRNA-205–directed transcriptional activation of tumor suppressor genes in prostate cancer. Cancer *116*, 5637-5649.

Markljung, E., Jiang, L., Jaffe, J.D., Mikkelsen, T.S., Wallerman, O., Larhammar, M., Zhang, X., Wang, L., Saenz-Vash, V., Gnirke, A., et al. (2009). ZBED6, a novel transcription factor derived from a domesticated DNA transposon regulates IGF2 expression and muscle growth. PLoS Biol. *7*, e1000256.

Matsui, M., Chu, Y., Zhang, H., Gagnon, K.T., Shaikh, S., Kuchimanchi, S., Manoharan, M., Corey, D.R., and Janowski, B.A. (2013). Promoter RNA links transcriptional regulation of inflammatory pathway genes. Nucleic Acids Res. *41*, 10086-10109.

Molina-Pinelo, S., Gutiérrez, G., Pastor, M.D., Hergueta, M., Moreno-Bueno, G., García-Carbonero, R., Nogal, A., Suárez, R., Salinas, A., Pozo-Rodríguez, F., et al. (2014). MicroRNA-dependent regulation of transcription in non-small cell lung cancer. PLoS One *9*, e90524.

Neilson, J.R., Zheng, G.X., Burge, C.B., and Sharp, P.A. (2007). Dynamic regulation of miRNA expression in ordered stages of cellular development. Genes Dev. *21*, 578-589.

Ohnishi, Y., Totoki, Y., Toyoda, A., Watanabe, T., Yamamoto, Y., Tokunaga, K., Sakaki, Y., Sasaki, H., and Hohjoh, H. (2012). Active role of small non-coding RNAs derived from SINE/B1 retrotransposon during early mouse development. Mol. Biol. Rep. *39*, 903-909.

Ohta, Y., Shichinohe, H., and Nagashima, K. (2002). Spinal cord compression due to extramedullary hematopoiesis associated with polycythemia vera—case report—. Neurol. Med. Chir. (Tokyo) *42*, 40-43.

Ørom, U.A., Nielsen, F.C., and Lund, A.H. (2008). MicroRNA-10a binds the 5′ UTR of ribosomal protein mRNAs and enhances their translation. Mol.

Cell *30*, 460-471.

Payer, L.M. and Burns, K.H. (2019). Transposable elements in human genetic disease. Nat. Rev. Genet. *20*, 760-772.

Peng, C., Wang, M., Shen, Y., Feng, H., and Li, A. (2013). Reconstruction and analysis of transcription factor–miRNA co-regulatory feed-forward loops in human cancers using filter-wrapper feature selection. PLoS One *8*, e78197.

Piriyapongsa, J. and Jordan, I.K. (2007). A family of human microRNA genes from miniature inverted-repeat transposable elements. PLoS One *2*, e203.

Piriyapongsa, J., Mariño-Ramírez, L., and Jordan, I.K. (2007). Origin and evolution of human microRNAs from transposable elements. Genetics *176*, 1323-1337.

Sawado, T., Igarashi, K., and Groudine, M. (2001). Activation of β-major globin gene transcription is associated with recruitment of NF-E2 to the β-globin LCR and gene promoter. Proc. Natl. Acad. Sci. U. S. A. *98*, 10226-10231.

Shivdasani, R.A. (2006). MicroRNAs: regulators of gene expression and cell differentiation. Blood *108*, 3646-3653.

Song, K.H., Li, T., Owsley, E., and Chiang, J.Y. (2010). A putative role of micro RNA in regulation of cholesterol 7α-hydroxylase expression in human hepatocytes. J. Lipid Res. *51*, 2223-2233.

Spivak, J.L. (2010). Narrative review: thrombocytosis, polycythemia vera, and JAK2 mutations: the phenotypic mimicry of chronic myeloproliferation. Ann. Intern. Med. *152*, 300-306.

Sun, W., Samimi, H., Gamez, M., Zare, H., and Frost, B. (2018). Pathogenic tau-induced piRNA depletion promotes neuronal death through transposable element dysregulation in neurodegenerative tauopathies. Nat. Neurosci. *21*, 1038-1048.

Suzuki, H.I., Young, R.A., and Sharp, P.A. (2017). Super-enhancer-mediated RNA processing revealed by integrative microRNA network analysis. Cell *168*, 1000-1014.e15.

Tsai, N.P., Lin, Y.L., and Wei, L.N. (2009). MicroRNA mir-346 targets the 5′-untranslated region of receptor-interacting protein 140 (RIP140) mRNA and up-regulates its protein expression. Biochem. J. *424*, 411-418.

Turner, M., Jiao, A., and Slack, F.J. (2014). Autoregulation of lin-4 microRNA transcription by RNA activation (RNAa) in C. elegans. Cell Cycle *13*, 772-781.

Ullu, E. and Tschudi, C. (1984). Alu sequences are processed 7SL RNA genes. Nature *312*, 171-172.

Wang, H., Tang, C., Na, M., Ma, W., Jiang, Z., Gu, Y., Ma, G., Ge, H., Shen, H., and Lin, Z. (2017). miR-422a inhibits glioma proliferation and invasion by targeting IGF1 and IGF1R. Oncol. Res. *25*, 187-194.

Wang, R., Zhang, S., Chen, X., Li, N., Li, J., Jia, R., Pan, Y., and Liang, H. (2018). CircNT5E acts as a sponge of miR-422a to promote glioblastoma tumorigenesis. Cancer Res. *78*, 4812-4825.

Wei, F., Yang, L., Jiang, D., Pan, M., Tang, G., Huang, M., and Zhang, J. (2020). Long noncoding RNA DUXAP8 contributes to the progression of hepatocellular carcinoma via regulating miR-422a/PDK2 axis. Cancer Med. *9*, 2480-2490.

Wei, W.T., Nian, X.X., Wang, S.Y., Jiao, H.L., Wang, Y.X., Xiao, Z.Y., Yang, R.W., Ding, Y.Q., Ye, Y.P., and Liao, W.T. (2017). miR-422a inhibits cell proliferation in colorectal cancer by targeting AKT1 and MAPK1. Cancer Cell Int. *17*, 91.

Wienholds, E. and Plasterk, R.H. (2005). MicroRNA function in animal development. FEBS Lett. *579*, 5911-5922.

Wu, L., Hu, B., Zhao, B., Liu, Y., Yang, Y., Zhang, L., and Chen, J. (2017). Circulating microRNA-422a is associated with lymphatic metastasis in lung cancer. Oncotarget *8*, 42173-42188.

Wu, Q., Qin, H., Zhao, Q., and He, X.X. (2015). Emerging role of transcription factor-microRNA-target gene feed-forward loops in cancer. Biomed. Rep. *3*, 611-616.

Xiao, M., Li, J., Li, W., Wang, Y., Wu, F., Xi, Y., Zhang, L., Ding, C., Luo, H., Li, Y., et al. (2017). MicroRNAs activate gene transcription epigenetically as an enhancer trigger. RNA Biol. *14*, 1326-1334.

Yang, W., Wang, J., Chen, Z., Chen, J., Meng, Y., Chen, L., Chang, Y., Geng, B., Sun, L., Dou, L., et al. (2017). NFE2 induces miR-423-5p to promote gluconeogenesis and hyperglycemia by repressing the hepatic FAM3A-ATP-Akt pathway. Diabetes *66*, 1819-1832.

Yuan, Z., Sun, X., Jiang, D., Ding, Y., Lu, Z., Gong, L., Liu, H., and Xie, J. (2010). Origin and evolution of a placental-specific microRNA family in the human genome. BMC Evol. Biol. *10*, 346.

Zhang, H., He, Q.Y., Wang, G.C., Tong, D.K., Wang, R.K., Ding, W.B., Li, C., Wei, Q., Ding, C., Liu, P.Z., et al. (2018a). miR-422a inhibits osteosarcoma proliferation by targeting BCL2L2 and KRAS. Biosci. Rep. *38*, BSR20170339.

Zhang, H.M., Kuang, S., Xiong, X., Gao, T., Liu, C., and Guo, A.Y. (2015a). Transcription factor and microRNA co-regulatory loops: important regulatory motifs in biological processes and diseases. Brief. Bioinform. *16*, 45-58.

Zhang, J., Yang, Y., Yang, T., Yuan, S., Wang, R., Pan, Z., Yang, Y., Huang, G., Gu, F., Jiang, B., et al. (2015b). Double-negative feedback loop between microRNA-422a and forkhead box (FOX) G1/Q1/E1 regulates hepatocellular carcinoma tumor growth and metastasis. Hepatology *61*, 561-573.

Zhang, Y., Wan, J., Liu, S., Hua, T., and Sun, Q. (2018b). Exercise induced improvements in insulin sensitivity are concurrent with reduced NFE2/miR-432-5p and increased FAM3A. Life Sci. *207*, 23-29.

Zhou, X., Duan, X., Qian, J., and Li, F. (2009). Abundant conserved microRNA target sites in the 5′-untranslated region and coding sequence. Genetica *137*, 159-164.

Zhou, Y., Ferguson, J., Chang, J.T., and Kluger, Y. (2007). Inter-and intra-combinatorial regulation by transcription factors and microRNAs. BMC Genomics *8*, 396.

Zou, Y., Chen, Y., Yao, S., Deng, G., Liu, D., Yuan, X., Liu, S., Rao, J., Xiong, H., Yuan, X., et al. (2018). MiR-422a weakened breast cancer stem cells properties by targeting PLP2. Cancer Biol. Ther. *19*, 436-444.